

Specific Ion Effects of Divalent Cations on the Formation and Properties of Polyelectrolyte Multilayers

Mia Mesić[#],^[a] Tin Klačić,^[a] and Davor Kovačević^{*[a]}

Multilayer films made of strong polyelectrolytes poly(diallyldimethylammonium chloride) and poly(sodium 4-styrenesulfonate) were built-up on silicon wafer using the layer-by-layer method. The films were built-up in the presence of various divalent cations (Mg^{2+} , Ca^{2+} , Sr^{2+} , Ni^{2+} , Zn^{2+} , and Cu^{2+}) to examine how the nature of cations affects the properties of the film. The results have shown that the thickness, morphology, and roughness of films prepared in the presence of transition metal cations are not significantly different. In contrast, these properties varied

for multilayers prepared in the presence of alkaline earth metal cations. The difference in the ion-specific behavior of these two classes of cations was explained by the difference in the hydration of these ions and by the bridging of polyelectrolyte chains with ions. While transition metal cations have similar hydration parameters, alkaline earth cations have different degrees of hydration and a better ability to form bridging bonds with polyelectrolyte monomers.

1. Introduction

Polyelectrolyte multilayers (PEMs) are polymeric ultrathin films commonly prepared on a solid surface through layer-by-layer (LbL) technique.^[1] The LbL technique consists of alternative dipping of a substrate in solutions of oppositely charged polyelectrolytes. In that way, PEMs are built-up on a substrate surface in a step-by-step fashion. Nowadays, PEMs offer a wide range of applications in the fields of anticorrosives,^[2] membranes,^[3,4] flame retardants,^[5,6] humidity sensors,^[7] bactericides,^[8,9] and drug delivery.^[10,11] The reason for a high number of possible applications of PEMs lies in the fact that their structure and properties can be very precisely adjusted by varying preparation conditions such as ionic strength and pH of dipping solutions,^[12–15] polyion concentration,^[16,17] temperature,^[18,19] and substrate type.^[20,21]

In addition to the mentioned parameters, the type of supporting electrolyte present in polyelectrolyte assembly solutions also affects the properties of LbL films. For monovalent anions, it was shown that the properties of PEMs, such as film thickness, roughness, stiffness, wettability, and degree of swelling, correlate well with the anion position in the Hofmeister series.^[22–27] In that context, several attempts have been made to relate the order of anions in Hofmeister series with some physical quantity (anion's size and hydration entropy, anion's polarizabil-

ity, and Jones-Dole viscosity B coefficient, to name a few).^[22–25] Although no such unique quantity has been found, the effect of monovalent anions on PEM properties was often explained phenomenologically by the difference in binding affinity of anions to the oppositely charged sites on polyelectrolyte chains.^[28] In this sense, large and poorly hydrated monovalent anions (chaotropic anions) have a considerable higher ability to screen the charged monomers of polycations in the solution than the small anions with a well-ordered large hydration shell (cosmotropic anions). Consequently, in the solution of chaotropic anions, polycation molecules will be present in a more compact conformation than in the solution of cosmotropic anions due to the more reduced intrachain electrostatic repulsions. Adsorption of such globular macroion chains to a surface leads to thicker films with higher surface roughness.

As mentioned earlier, the Hofmeister series provides a general model for explaining the effect of monovalent anions on the properties of multilayer films. However, it was shown by Dressick and co-workers^[29] that the Hofmeister series is not enough to explain the influence of divalent anions on the properties of PEMs. They investigated the effect of divalent anions (SO_4^{2-} , HPO_4^{2-} , and organic dicarboxylates) on the formation of PEMs built-up from sodium polystyrenesulfonate (PSS) and poly(allylamine hydrochloride) (PAH). The obtained differences in the thickness and surface roughness of the PSS/PAH film prepared with dipping solutions of various divalent anions were explained by the difference in the bridging ability of PAH chains with the respective anions. As pointed out by the authors, this bridging ability of the anions is dominated by these separation, rigidity, and angle between the discrete negatively charged sites in the dianion structure.

In contrast to the anion effect, the influence of the nature of cations on PEM formation and properties is much less pronounced. For example, Wong et al.^[25] investigated the impact of monovalent cations and anions and their concentrations in the dipping solutions on the thickness and roughness of multilayers deposited from PSS and poly(diallyldimethylammonium chloride) (PDADMAC) solutions. In the case of anions, they found

[a] M. Mesić[#], T. Klačić, D. Kovačević
 Division of Physical Chemistry, Faculty of Science,
 University of Zagreb, Horvatovac 102a, Zagreb 10000, Croatia
 E-mail: davor.kovacevic@chem.pmf.hr

[[#]] Present Address: Division of Materials Chemistry, Ruđer Bošković Institute,
 Bijenička cesta 54, 10,000 Zagreb, Croatia

Supporting information for this article is available on the WWW under
<https://doi.org/10.1002/slct.202501185>

© 2025 The Author(s). ChemistrySelect published by Wiley-VCH GmbH. This is an open access article under the terms of the [Creative Commons Attribution License](#), which permits use, distribution and reproduction in any medium, provided the original work is properly cited.

that specific ion effects become important above a critical anionic concentration of 0.1 mol dm^{-3} . However, in the case of cations, ion concentration of above 0.25 mol dm^{-3} was necessary to observe the measurable difference. In another study, Büscher and co-workers^[18] did not notice any significant difference in the thickness of PAH/PSS films prepared in the presence of KCl, NaCl, and CsCl even at salt concentration of 1.0 mol dm^{-3} . How is it that anions have such a superior effect on PEMs than cations? One of the possible explanations for the more pronounced anion-specific effect than the cation-specific effect was given by von Klitzing and colleagues.^[28] They suggested that the effect of anions is much greater than the effect of cations because anions have a much larger difference in polarizability than typical cations due to the greater variety of their diameter.

The less pronounced influence of monovalent cations on the LbL films was probably one of the main reasons that this type of research was not extended to divalent cations. According to our knowledge, there is not a single publication documented in the literature in which the influence of the type of divalent cations on the preparation and properties of PEMs was systematically investigated. In an attempt to fill that gap in the literature, the present article focuses on the effect of the type of divalent cations on the thickness, roughness, and wettability of PDADMAC/PSS multilayer. From one side, the PDADMAC/PSS system was selected for that purpose because it is a rigorously studied system^[30–32] of two strong polyelectrolytes with moderately weak intrinsic interactions susceptible to the influence of counterions.^[33] From the other side, the following salts have been chosen to study the effects of divalent cations on the properties of PDADMAC/PSS assembly: MgCl_2 , CaCl_2 , SrCl_2 , BaCl_2 , NiCl_2 , CuCl_2 , and ZnCl_2 . In this series of chloride salts, ions Mg^{2+} , Ca^{2+} , Sr^{2+} , and Ba^{2+} are the representatives of the alkaline earth metals, whereas Ni^{2+} , Cu^{2+} , and Zn^{2+} ions belong to transition metals. Both groups of these metal cations might give new opportunities to control the structure and properties of polyelectrolyte multilayers through specific ion effects.

2. Experimental Section

2.1. Materials

Single-side polished monocrystalline silicon wafer discs (orientation: $\langle 100 \rangle$, p-type doped with boron) of 150 mm diameter were obtained from Siltronic AG. The water solutions of poly(diallyldimethylammonium chloride) ($w = 29.6\%$, $M_w \approx 200\,000\text{--}350\,000 \text{ g mol}^{-1}$) and poly(sodium 4-styrenesulfonate) ($w = 20.2\%$, $M_w \approx 200\,000 \text{ g mol}^{-1}$) were purchased from Sigma Aldrich. All salts ($\text{CaCl}_2 \times 6\text{H}_2\text{O}$, CuCl_2 , MgCl_2 , BaCl_2 , ZnCl_2 , NiCl_2 , and SrCl_2) were also purchased from Sigma Aldrich and stored in a vacuum desiccator with anhydrous CaCl_2 as wetting agents due to hygroscopicity and reactivity with the atmosphere. Deionized water, which was used for all experiments, was prepared with a Millipore Mili-Q Plus 185 purification system and had a conductivity lower than $0.055 \mu\text{S cm}^{-1}$.

2.2. Dynamic Light Scattering (DLS)

A BI-90 Plus Particle Size Analyzer from Brookhaven Instruments Corporation was used for polyelectrolyte aggregate detection and

determination of the particle hydrodynamic diameters. The used instrument is equipped with a diode laser ($\lambda = 635 \text{ nm}$) and a detector positioned at an angle of 90° relative to the incident radiation. The experiments were performed at a temperature of 25°C with 2 mL of PSS solutions ($c_m = 0.01 \text{ mol dm}^{-3}$) containing chloride salts of different divalent cations ($c = 0.1$ or 0.5 mol dm^{-3}). After dissolving a certain amount of salt in the PSS solution, the pH value of the solution was adjusted to 4.0 using an aqueous HCl solution ($c = 1 \text{ mol dm}^{-3}$). The Brownian motion of particles present in the prepared solutions was traced and analyzed using the BIC Particle Sizing Software (version 4.1) supplied with the instrument. The obtained values of the effective hydrodynamic diameter are expressed in the manuscript as the mean values of ten measurements (\pm standard deviation).

2.3. Preparation of Polyelectrolyte Multilayers

The PDADMAC/PSS multilayers were prepared on Si wafers by the LbL method.^[1] Before PEM preparation, Si discs were cut into plates of $1 \times 1 \text{ cm}^2$ or $5 \times 1 \text{ cm}^2$ dimensions and cleaned in *Piranha* solution for about 1 h. After that, the substrates were rinsed with deionized water and then dried in the stream of inert argon gas (5.0, Messer). The *Piranha* solution was prepared by mixing of concentrated H_2SO_4 (Lach-Ner) and H_2O_2 (Kemika) in 3:1 ratio. The alternating immersion of the silicon substrate into polycation and polyanion solution was conducted either manually or with the aid of a dip coating robot (model DR-3, Riegler & Kirstein GmbH). In both film preparation procedures, the concentration of polyelectrolyte repeating units in solutions was 0.01 mol dm^{-3} , and the concentration of background salt was 0.1 mol dm^{-3} . Salts were dried at 120°C for about 3 h before dissolving them in polymer solutions. The pH value of polyelectrolyte solutions was adjusted to 4.0 ± 0.1 with a 1.0 mol dm^{-3} HCl solution (Merck). That pH value was chosen because all investigated cations are present in the + II oxidation state at that pH.^[34]

For the determination of pH value, a pH meter (913 pH Meter, Metrohm) with combined electrode was calibrated with standard buffers of pH 3.0, 5.0, 7.0, and 9.0. Since at pH = 4.0 the surface of silica is negatively charged,^[21,35] the first adsorbed polyelectrolyte was polycation PDADMAC. In the case of manual film preparation, the Si plate of $1 \times 1 \text{ cm}^2$ dimensions was attached with tweezers to a metal stand and immersed for 5 min in a polyelectrolyte solution. After the deposition cycle was finished, the silicon substrate was immersed three times for 1 min in 25 mL of deionized water and then blow-dried in the stream of argon. The preparation process was repeated for ten cycles to achieve a ten-layer film. On the contrary, the LbL deposition robot was used to prepare films containing of 30 layers. For that purpose, the $5 \times 1 \text{ cm}^2$ silicon plate was immersed for 5 min in a polyelectrolyte solution, rinsed three times for 1 min in the bath filled with deionized water, and blow-dried in the stream of inert argon gas. The automatic process of PEM preparation was controlled by Dipp3d-Win software (Version 1.3). For simplicity, prepared films are denoted in a text as (PDADMAC/PSS) x where x is the number of bilayers.

2.4. Ellipsometry

The thickness of the polyelectrolyte films was determined using L116B-USB ellipsometer from Gaertner. Ellipsometric measurements were performed under ambient conditions using a He-Ne laser of a monochromatic beam at 632.8 nm. The reflection angle of the laser beam, in relation to the normal of the sample, was set to 70° . Data on the thickness of the films were generated based on the set model in the GEMP program (Gaertner Ellipsometry Mea-

surement Program, series: 8.071). The model assumed a system with three phases consisting of the substrate, the film, and the surrounding atmosphere (air) whose refractive index^[36] is $n = 1.000$. While the refractive index of the silicon wafer (Si/SiO_x) was determined for each substrate before measuring the PEM thickness, the refractive index of the film was fixed to^[37] $n = 1.55$. The thickness of the multilayer was averaged based on measurements made at ten different positions on the surface.

2.5. Atomic Force Microscopy (AFM)

AFM measurements were performed at ambient conditions using Bruker device MultiMode 8. Scanning of the samples was performed in tapping mode to prevent contamination of the AFM probe with polymeric material. For the stated purpose, NCHV-A silicon probes (Bruker) were used. These probes have a rectangular cantilever of 125 μm length and 33 μm width, with a nominal resonance frequency of 320 kHz and a nominal constant of 42 N m^{-2} . The tip of the used probe has a nominal radius of curvature of 8 nm. In most of the measurements, the AFM scanning area was 5 $\mu\text{m} \times 5 \mu\text{m}$, the scanning angle was 0° or 90°, the scanning speed was 1.0 Hz, and the resolution of the image was 512 px \times 512 px. Just before the measurement, the exact resonance frequency of the used AFM probe was determined by auto-tuning. Data during measurements were monitored and collected in the program NanoScope Scan 9.7 and later analyzed in the program NanoScope Analysis 2.0.

AFM images of the multilayer surface were collected at five different locations. The root mean square (RMS) roughness is expressed in the text by the R_q value, which was obtained by analyzing the recorded images. The film thickness was determined by making a scratch on the silicon surface with very sharp tweezers to remove the soft polyelectrolyte multilayer. Then, a scanning of the scratch was made, and the obtained AFM image was processed in the Gwyddion program (64-bit version 2.60), where the average thickness of the film and the standard deviation of the arithmetic mean were obtained.

2.6. Contact Angle Measurements

Contact angle measurements were performed using the Attension Theta Lite tensiometer (Biolin Scientific). Before the measurement, the tensiometer was calibrated with a tungsten carbide ball. For calibration, experiments, and data analysis OneAttension program (version 4.1.3) was used. Contact angle measurements were carried out using the sessile drop method^[38] under ambient conditions. A drop of deionized water ($V \approx 4 \mu\text{L}$) was placed on the surface of the sample with the automatic pipette, and the recording of photos (resolution: 1216 px \times 800 px) by a CCD camera automatically started using the trigger option in the software. The recording lasted 10 seconds with a frequency of 20 photos per second. The photographs were stored on the computer and the contour of the droplet on the substrate was analyzed by the Young-Laplace equation^[38] on the sample of 62 photographs between the third and the sixth second of recording. For each photo, the contact angle on the left and right side of the droplet was determined, averaged, and the value of the contact angle was calculated. The average value of the contact angle for the prepared multilayers was obtained based on five measurements at different locations on the film surface.

3. Results

The aim of our study was to investigate how the presence of different divalent cations in deposition solutions affects the

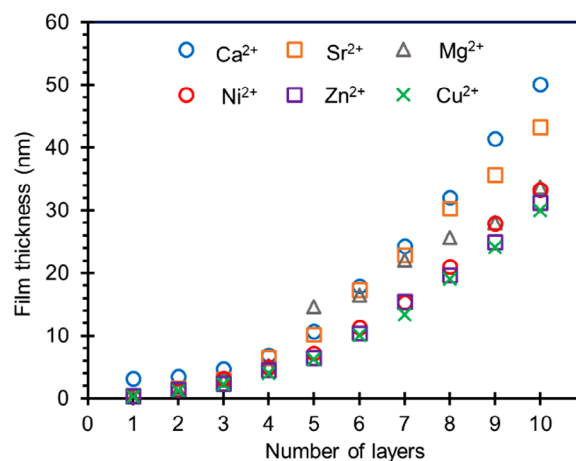


Figure 1. Ellipsometrically determined thickness of PDADMAC/PSS multilayers as a function of a number of deposited polyelectrolyte layers on the Si substrate. Multilayers were prepared in the presence of different divalent cations. Maximum standard error of all measurements is 0.6 nm.

formation and properties of PDADMAC/PSS multilayers. Before conducting the experiments with polyelectrolyte films, it was necessary to determine at which salt concentration the preparation of PEMs would be carried out. On one hand, the salt concentration in the solution should be high enough to observe the ion-specific effects. On the other hand, the salt concentration should be low enough not to cause polyelectrolyte aggregation. To determine the optimal background salt concentration for the experiments, we prepared PSS solutions in different supporting electrolytes of 0.1 and 0.5 mol dm^{-3} concentration. The visual inspection of the prepared solutions (Figure S1) and the DLS measurements (Table S1) indicated that aggregates are present in most of the solutions at a salt concentration of 0.5 mol dm^{-3} . In contrast, at 0.1 mol dm^{-3} salt concentration, the aggregates were detected only in the solution containing Ba²⁺ ions (Figure S2 and Table S2). Therefore, PEMs were prepared at 0.1 mol dm^{-3} electrolyte concentration in the presence of all investigated background salts except BaCl₂.

3.1. Thickness of Multilayer Films

In order to determine the thickness of the investigated PDADMAC/PSS multilayers prepared in an environment of different divalent cations, ellipsometry and AFM were used. In the first phase of the study, the growth regime of each prepared multilayer, which had a total of ten layers, was monitored ellipsometrically. The obtained results are shown in Figure 1. The film prepared in the presence of Ca²⁺ ions reached the thickness of 50 nm, followed by the film with Sr²⁺ ions having the thickness of 43 nm, whereas the thinnest film of 33 nm was obtained in the presence of Mg²⁺ ions. It is noticeable that the thickness of the ten-layer films prepared with d-block elements is around 30 nm, and there are no significant differences among them. From Figure 1, it is visible that the growth of all films is exponential. Also, the differences in the increase of film thicknesses

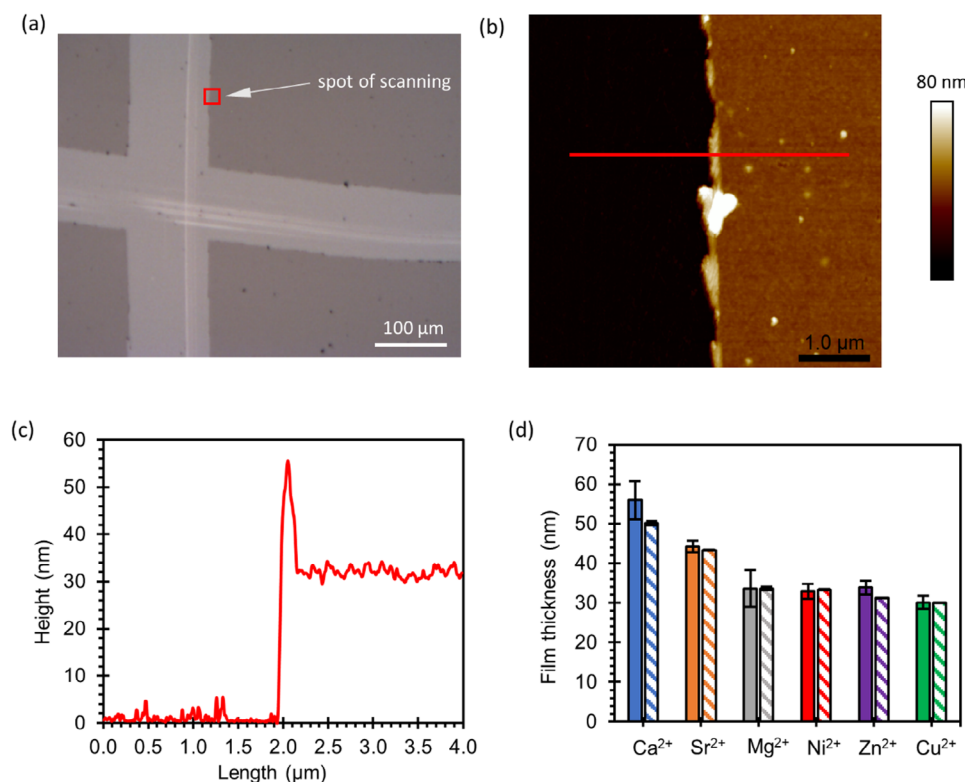


Figure 2. (a) The digital optical microscopy image and (b) the AFM image of the surface area where the (PDADMAC/PSS)₅ multilayer, built-up in the presence of ZnCl₂, was removed from the substrate surface with sharp tweezers. (c) The height profile crosses the red line designated in the AFM image. (d) Comparison between AFM (solid columns) and ellipsometric (patterned columns) thickness of (PDADMAC/PSS)₅ multilayers prepared in the presence of different background cations.

are more expressed in the presence of cations of alkaline earth metals than in the presence of cations of transition metals.

In addition to the ellipsometric measurements, AFM was used to determine the thickness of (PDADMAC/PSS)₅ multilayers. For that purpose, the film was removed from one part of the substrate by making a scratch on the surface with sharp tweezers. The surface was then scanned on the boundary between the film and the substrate with AFM to obtain the height profile. In the end, numerous height profiles were collected and the film thickness was calculated. The example of the area where PEM was removed from the surface, as well as the example of the height profile, is shown in Figure 2a,c.

In Figure 2a, bright lines represent parts of the surface from which the LbL assembly has been removed. If the area along the very edge of these lines is scanned with AFM, a flat surface of the substrate and the rougher surface of the PEM can be observed (Figure 2b). Next to the substrate/film edge itself, protrusions can be noticed on the surface of the PEM (Figure 2b,c). Such protrusions on the surface can also be observed in the AFM images published by others (for example, see Figure 1 in Doodoo et al.).^[32] We suppose that they are made as the tip of the tweezers passes over the surface and removes the excess polymer material to the side. Figuratively, this process is similar to removing snow from the road with a snowplow. Therefore, it should be pointed out that protrusions were not taken into account during PEM thickness determination.

The comparison between AFM and ellipsometric thickness of (PDADMAC/PSS)₅ multilayers prepared in the presence of different background cations is depicted in Figure 2d. As it can be seen, the trend in thickness determined by AFM is the same as the one measured by the ellipsometer. In the case of alkaline earth metals, we see that film thickness increases in order Mg²⁺ < Sr²⁺ < Ca²⁺, whereas in the case of d-block elements, no differences were observed. It is also worth mentioning that the thickness of LbL film prepared in the presence of Mg²⁺ is of the same order as the thickness of PEMs prepared in the presence of transition metal cations. Not only that the trend in thicknesses determined by ellipsometry and AFM match well, but also the absolute values of film thicknesses are comparable. Good agreement in film thicknesses determined by AFM and ellipsometry was also obtained by Salomäki and co-workers^[22] when studying the ion-specific effect for anions.

On the basis of the results obtained so far, it was noticed that the type of alkaline earth metal affects the PDADMAC/PSS film thickness, and the type of transition metal does not. However, it is possible that there is a difference in thickness between the films prepared in the presence of Ni²⁺, Zn²⁺, and Cu²⁺ ions, but it is not clearly visible due to the insufficient number of deposited polymer layers on the surface. Therefore, we prepared 15 PDADMAC/PSS bilayers on a Si wafer in the presence of different divalent cations using LbL robot. The thickness of prepared (PDADMAC/PSS)₁₅ multilayers, obtained by ellipsometry and AFM, is shown in Figure 3. The results of both methods

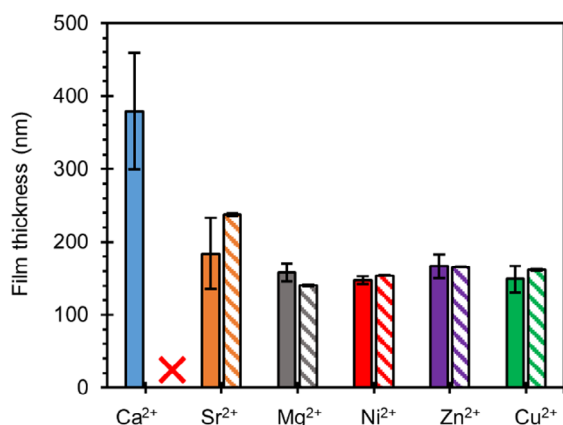


Figure 3. AFM (solid columns) and ellipsometric (patterned columns) thickness of (PDADMAC/PSS)₁₅ films prepared in the presence of different background cations. X denotes that the thickness of PEM prepared in the presence of Ca²⁺ ions was not possible to determine with an ellipsometer.

match well and indicate that the trend in the film thickness is the same as the one with 10-layer films. PEMs prepared in the presence of transition metals have very similar thicknesses, whereas the thickness of films prepared in the presence of alkaline earth metals increases in order: Mg²⁺ < Sr²⁺ < Ca²⁺. For a film built-up in the presence of Ca²⁺ ions, it was impossible to determine the thickness using ellipsometry due to the limitations of the method. The first limitation is related to the maximum film thickness that can be measured with the used ellipsometer ($d_{\max} \approx 300$ nm) and the second is related to the high roughness of the surface, and therefore the laser beam is scattered.

3.2. Topography and Roughness of PEM Surfaces

In addition to the film thickness, AFM was also used to study how the presence of divalent cations in assembly solutions affects the morphological properties and surface roughness of the studied multilayers. In the beginning, the surfaces of the (PDADMAC/PSS)₅ and (PDADMAC/PSS)₁₅ multilayers were recorded using a digital optical microscope (Figure S3). Even on a large scale, protrusions and high surface roughness of the films prepared in the presence of CaCl₂ and MgCl₂ can be seen, whereas the film with SrCl₂ has the smoothest surface. Films formed in the presence of NiCl₂, ZnCl₂, and CuCl₂ have very similar surface morphology.

The surface of prepared films was scanned using the tapping mode of AFM to obtain a more detailed insight into the surface morphology and roughness of films on a smaller scale. The resulting AFM images are shown in Figure 4. The biggest differences in surface morphology and roughness can be observed for PEMs prepared in the presence of alkaline earth metals, whereas there are no excessive differences in morphology and roughness in the case of d-block elements. From the AFM images, it can be seen that PEMs obtained in the presence of CaCl₂ have a worm-like surface, whereas films formed in the presence of SrCl₂ have a granular morphology. Furthermore, (PDADMAC/PSS)₅ film prepared with MgCl₂ has cavities on the surface that are not

seen on the surface of PEM with 30 layers. (PDADMAC/PSS)₅ multilayers prepared in the presence of nickel(II), zinc(II), and copper(II) chloride have very similar granular morphologies and smooth surfaces. The similarity in surface topography of PEMs prepared in the presence of these background salts is also visible for 30-layer films. However, these films have a worm-like surface structure.

By additional image processing, the surface roughness of (PDADMAC/PSS)₅ and (PDADMAC/PSS)₁₅ multilayers prepared with different supporting electrolytes was obtained (Figure 5). It is immediately visible from the results that PEMs with 30 polyelectrolyte layers have higher roughness than multilayers with 10 layers. It is not uncommon that thicker PEMs with a higher number of deposited layers have a higher surface roughness.^[32,39] By comparing the average R_q values of (PDADMAC/PSS)₅ multilayers (Figure 5a), it can be seen that the surface of the film prepared with Ca²⁺ ions is almost seven times rougher than the surface of the film built-up with Sr²⁺ ions and 1.8 times rougher than the surface of the film prepared with Mg²⁺. Films prepared with d-block elements have very similar roughness, and considering the roughness values are below 3 nm, they belong to the category of extremely smooth surfaces. From Figure 5b, it is visible that the 30-layer film obtained with Ca²⁺ ions is the roughest, followed by the film built-up in the presence of Sr²⁺ ions, whereas the smoothest film formed with earth alkaline cations is the multilayer with Mg²⁺ ions. For transition metals, slight differences in R_q values are visible, with PEM prepared in NiCl₂ deviating the most from the other two background salts.

3.3. Wettability of PEMs

The wettability of the film surface was determined by contact angle measurements using the sessile drop method. The change in the contact angle of PDADMAC/PSS multilayers prepared in the presence of various background salts was monitored after each adsorbed polyelectrolyte layer (Figure 6) because of the expected layer-to-layer contact angle oscillations. According to the literature, the surface of pure silicon has a contact angle of about 22°. [21] After adsorption of the first PDADMAC layer, the surface of the Si substrate became slightly more hydrophilic ($\theta \approx 10^\circ$) for all used background salts except for CaCl₂. In that case, the contact angle increased to 35°. Further successive adsorption of PSS and PDADMAC layers led to a zigzag change of contact angle, with PSS-terminating film being more hydrophobic than PDADMAC-terminating film. It is well known from the literature that the contact angle of LbL films changes with a number of adsorbed polyelectrolyte layers in that kind of pattern.^[40–42] If absolute values of contact angles are compared for PEMs prepared in different supporting electrolytes, no significant differences can be observed. The only exception is the film prepared in the presence of Mg²⁺ cations. The contact angle of that film with 5, 6, 7, 8, and 9 layers is significantly higher than that prepared in other background salt. One possible explanation for that result could be porous film morphology observed with AFM (Figure 4), as air of a hydrophobic nature can be trapped in the pores.

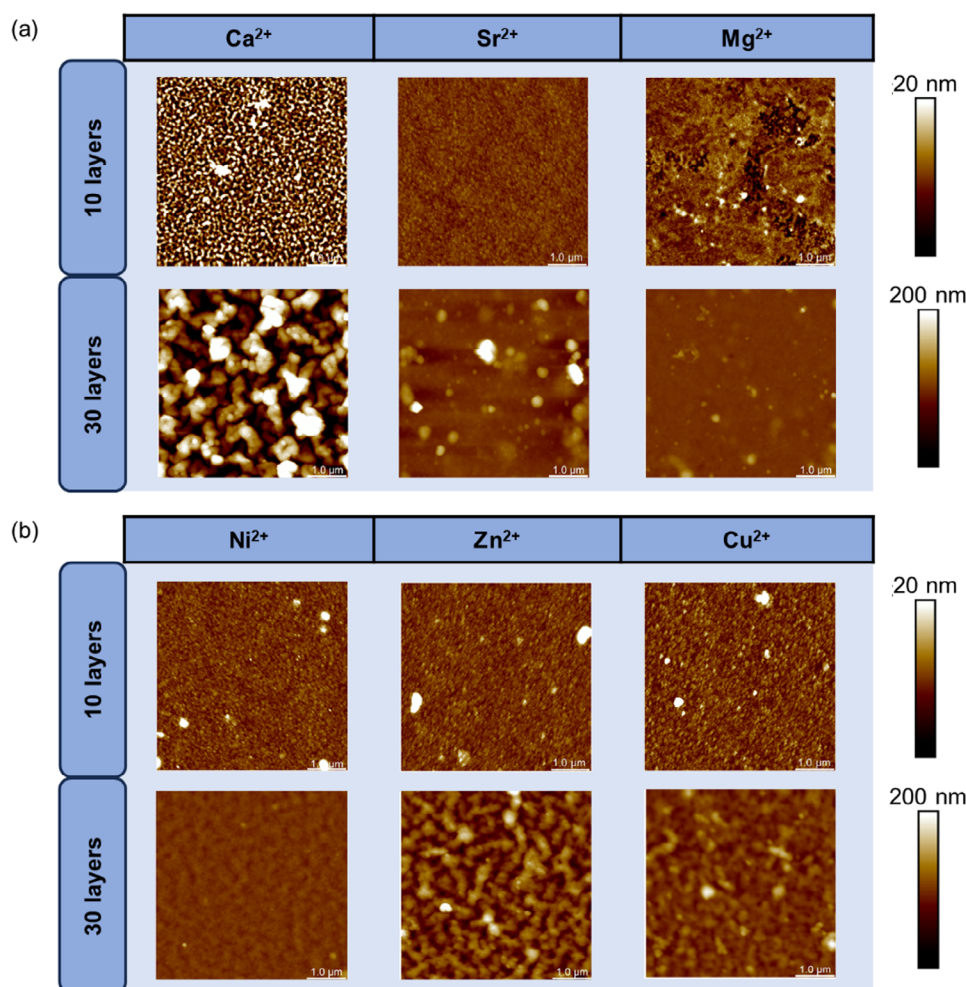


Figure 4. AFM images ($5 \times 5 \mu\text{m}^2$) of (PDADMAC/PSS)₅ and (PDADMAC/PSS)₁₅ multilayers built-up in the presence of (a) alkaline earth cations and (b) transition metal cations.

Figure 7 shows the influence of different divalent cations on the water contact angle of (PDADMAC/PSS)₁₅ multilayer prepared with the LbL robot. For comparison, in Figure 7, the contact angles of films with ten layers are given. If we take a closer look, it is visible that there is not an excessive difference in the contact angle of PEMs with 10 and 30 layers, as well as between PEMs prepared in the presence of different chloride salts. The surface of all the formed films is hydrophilic with a contact angle between 10° and 30°.

4. Discussion

In this study, we investigated how the type of divalent cation present in the assembly solution affects the thickness, roughness, and wettability of the PDADMAC/PSS multilayer. For convenience, the obtained results are summarized in Scheme 1. The thickness and surface roughness of both (PDADMAC/PSS)₅ and (PDADMAC/PSS)₁₅ films prepared in the presence of transition metal cations were not significantly different. In contrast, these properties differed for multilayers prepared in the presence of alkaline earth metal cations with the thickness and roughness

of films increasing in order: $\text{Mg}^{2+} < \text{Sr}^{2+} < \text{Ca}^{2+}$. Interestingly, the choice of background cation did not excessively influence the wettability of the prepared PEMs. Hence, the contact angle for all films was very similar. “Why does the type of alkaline earth cation affect the properties of the multilayer, but the type of transition metal does not, and why does the thickness and roughness of the film increase in the sequence $\text{Mg}^{2+} < \text{Sr}^{2+} < \text{Ca}^{2+}$?”; these are just some of the questions whose answers will be discussed afterward.

In general, the specific effect of ions on the formation and properties of PEMs is explained by the different abilities of ions to screen the free charges of polyions in solution.^[22,43,44] As a result of charge screening, the number of counterion-polyelectrolyte pairs increases, the monomer-monomer repulsions decrease, and the macromolecule adopts a more coiled form. That leads to polyelectrolyte deposition at the surface charge compensation, and thicker films with higher surface roughness are formed. It is believed that the driving force for this self-assembly process is the increase in entropy caused by the release of water molecules and counterions associated to polyelectrolyte chains as polycation and polyanion interact.^[45,46] The

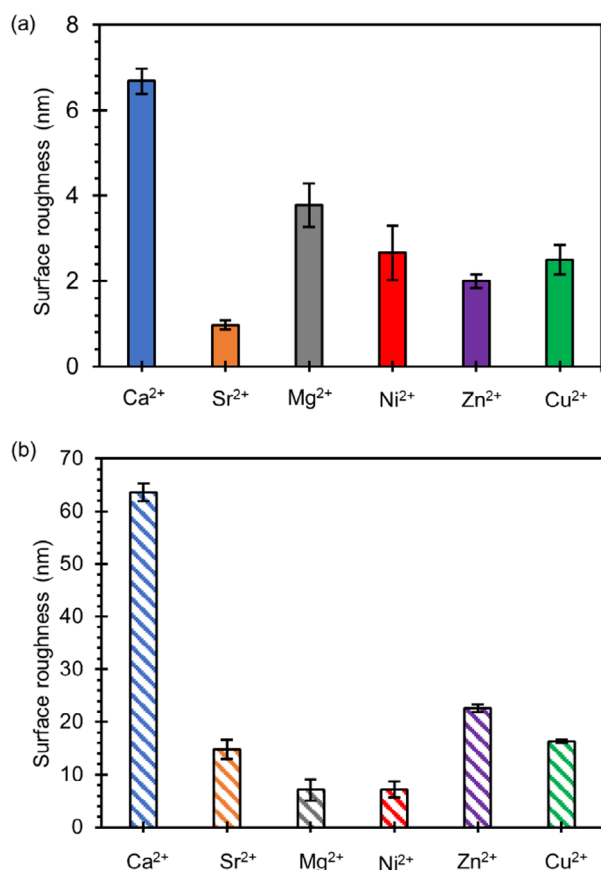


Figure 5. Surface roughness of (a) Si-(PDADMAC/PSS)₅ and (b) Si-(PDADMAC/PSS)₁₅ multilayers built-up in the presence of various divalent cations.

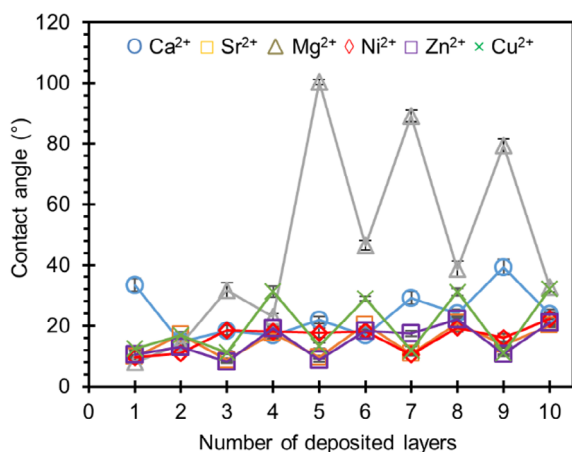


Figure 6. Contact angle of PDADMAC/PSS multilayers prepared in the presence of different divalent cations presented as a function of the number of layers. Odd numbers represent film when PDADMAC is the last layer, and even numbers represent film when PSS is the last layer.

formed multilayers are often named “frozen” structures because they represent metastable states that are kinetically trapped. Therefore, it is reasonable to assume that the type of background salt is the most important during the adsorption step because the polyelectrolyte-counterion binding constant is the one that exhibits ion specificity.

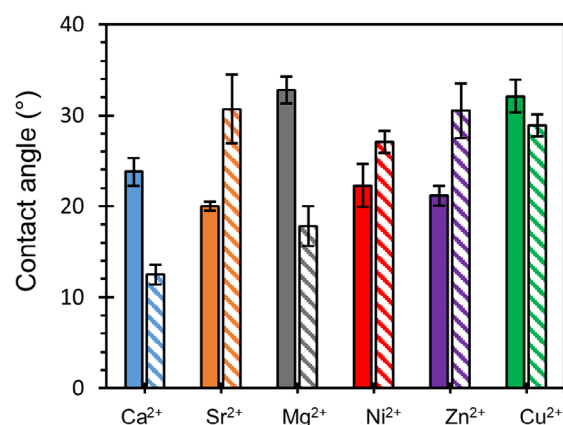
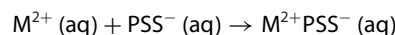


Figure 7. Contact angle of (PDADMAC/PSS)₅ (solid columns) and (PDADMAC/PSS)₁₅ (patterned columns) multilayers prepared in the presence of different divalent cations.

In solution, monodentate binding of divalent cations (M^{2+}) to PSS⁻ monomeric units can be represented by following equation.



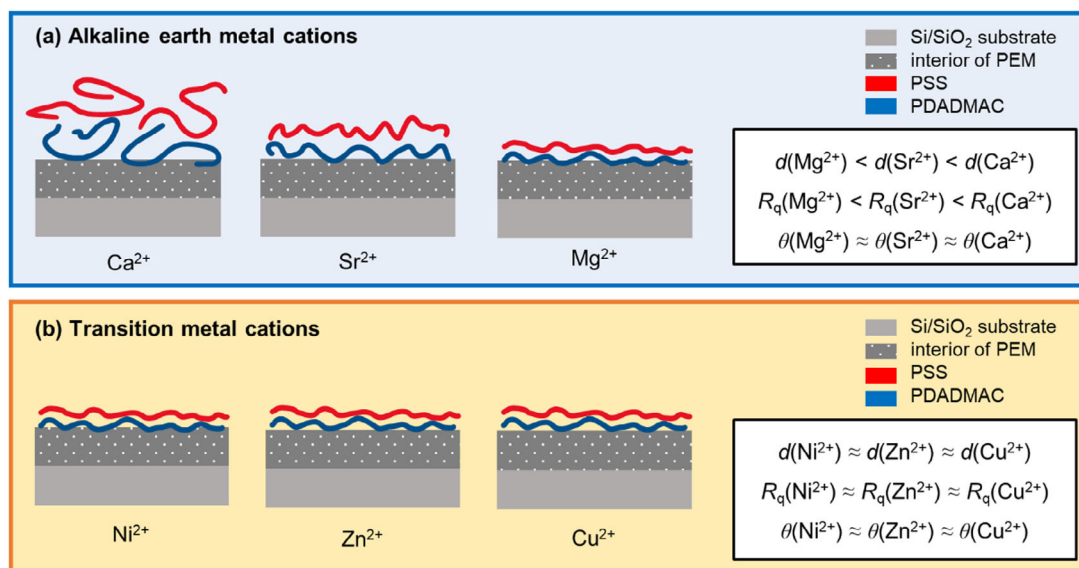
And bidentate binding by following equation.



In one of our previous studies,^[47] we conducted a potentiometric titration of $\text{Na}^{+}\text{PSS}^{-}(\text{aq})$ with a water solution of $M(\text{ClO}_4)_2$ ($M = \text{Mg}, \text{Sr}, \text{and Ba}$) using the sodium ion-selective electrode. From the results of those measurements, we found that divalent cations are generally bound to the PSS chain in a 1:2 ratio (2 monomer units of PSS per one cation). In that sense, one can conclude that the binding of divalent cations to PSS is more efficient than monovalent cations. To support this statement, the results of research performed by Warszyński and colleagues^[48] should be mentioned. They have demonstrated that the mass and thickness of the PDADMAC/PSS multilayer are higher when the polyelectrolytes are deposited in the presence of MgCl_2 than in the presence of NaCl .

For binding of cations to PSS repeating units, both partial/full desolvation of ions and partial/full desolvation of charged functional groups on the polymer chain are necessary. Consequently, differences in the fraction of bound counterions are to be expected considering the differences in their hydration. Table 1 depicts various hydration parameters of selected divalent cations.

From Table 1, we can see that the values of all parameters are very similar for transition metal cations. That is why we do not see excessive differences in thickness, roughness, morphology, and contact angle values of films prepared with NiCl_2 , ZnCl_2 , and CuCl_2 . Moreover, the Mg^{2+} ion has similar hydration parameters as transition metal cations, which could explain the comparable properties of PEMs prepared in the presence of that cation and cations of d-block elements. Contrary to the transition metal cations, the hydration parameters of alkaline earth cations are significantly different (Table 1). That difference in hydration of



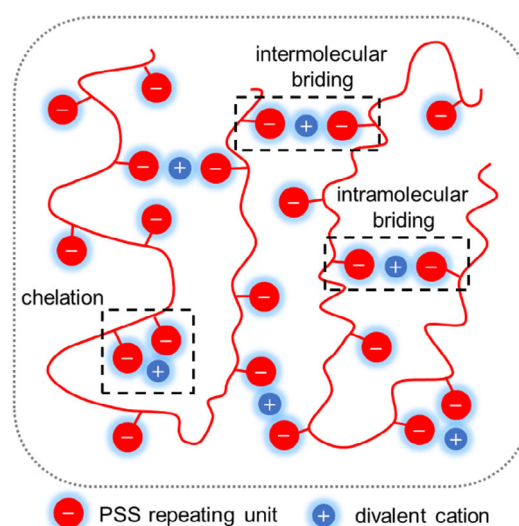
Scheme 1. Representations of PDADMAC/PSS multilayers build-up in the presence of different (a) alkaline earth cations and (b) transition metal cations. The insets show the relationship between thickness (d), roughness (R_q), and contact angle (θ) of the films prepared in the presence of different supporting electrolytes.

Table 1. Hydrodynamic radius (r_{hyd}), number of water molecules in the hydration shell (n), changes in hydration enthalpy (ΔH_{hyd}), entropy (ΔS_{hyd}) and Gibbs energy (ΔG_{hyd}) of the selected divalent cations. Ion parameters were taken from data published by Marcus.^[49]

Ion	r_{hyd} (pm)	n	$-\Delta H_{\text{hyd}}$ (kJ mol ⁻¹)	$-\Delta S_{\text{hyd}}$ (J K ⁻¹ mol ⁻¹)	$-\Delta G_{\text{hyd}}$ (kJ mol ⁻¹)
Mg ²⁺	299	10.0	1945	350	1830
Ca ²⁺	271	7.2	1600	271	1505
Sr ²⁺	263	6.4	1470	261	1380
Ba ²⁺	254	5.3	1330	224	1250
Ni ²⁺	302	10.4	2115	370	1980
Zn ²⁺	297	9.6	2120	339	2010
Cu ²⁺	295	9.4	2070	337	1955

Mg²⁺, Ca²⁺, and Sr²⁺ cations could reflect the difference in the observed thickness and roughness values of the PDADMAC/PSS films prepared in the presence of those cations. In Table 1, the Ba²⁺ ion is also included, although no measurements were made with it due to the formation of aggregates in the solutions. However, these aggregates indicate that the association of Ba²⁺ ions to PSS segments could be the most pronounced between all investigated divalent cations.

It is possible that in the case of the binding of well-hydrated ions (such as Ni²⁺, Zn²⁺, Cu²⁺, and Mg²⁺ cations), the bound ions retain the primary and even the secondary solvation sphere. That kind of indirect binding of counterions at greater distances from the polyelectrolyte chain should be significantly less specific than direct binding. In the case of weakly hydrated counterions (such as Ca²⁺, Sr²⁺, and Ba²⁺ cations), the hydration shell has higher polarizability and can be easier adapted to the environment, for example, to the polyion. That might lead to the stronger attraction between the counterion and PSS with direct



Scheme 2. Type of bonding of divalent cations to PSS repeating units in solution. Non-bonded divalent cations are not present in the scheme for simplicity.

contact ion pair formation resulting in stronger chain coiling due to the reduction in intrachain repulsion. Such a process, in the case of multilayers, leads to the increase in film thickness and surface roughness.

Another significant parameter that influences the conformation of polyelectrolytes in solution is the type of bonding of divalent cations to PSS repeating units. In general, we can distinguish two structural types of binding of divalent cations to the charged monomer units of PSS: chelate binding and bridging binding (Scheme 2). While chelate binding of cations implies positioning of ions between two adjacent PSS monomer groups, bridging bonding refers to the connection of two PSS groups that are located further apart on the same polymer chain

("intramolecular bridging") or on two neighboring ones ("intermolecular bridging"). From a molecular point of view, bridging polyelectrolyte units with ions has a more significant and far-reaching effect on the polyelectrolyte conformation than chelate ion binding. This means that even ions that have weak binding affinity to the PSS will be able to significantly affect the conformation of the polyion in solution, and consequently the properties of the PEMs, if they are associated to PSS monomer units by bridging. For example, we expected that less hydrated Sr^{2+} ions would condense more to the PSS segments than more hydrated Ca^{2+} ions. However, we experimentally observed that films prepared with CaCl_2 are significantly thicker and rougher than the films prepared with SrCl_2 (Figures 3 and 5). Such a result can be explained by a higher proportion of bridging bonds between PSS monomers in the case of Ca^{2+} than in the case of Sr^{2+} ions.

The importance of the ion-bridging effect on the PEM properties was also recognized by studies of other groups. In these studies,^[29,50,51] Lbl films were prepared with monovalent counterions and then exposed to solutions of divalent ions. For example, Wei et al.^[50] prepared the PDADMAC/PSS multilayer in NaNO_3 solution, which after exposure to $\text{Cu}(\text{NO}_3)_2$ solution reduced its thickness due to, as the authors explained, the cross-linking of PEM by Cu^{2+} ions. As they obtained similar results with other divalent nitrate cations, they concluded that this effect is not specific to a particular cation. In addition, Silva and coworkers^[51] came to the same conclusion after immersing the PAH/PSS film in a solution of $\text{Ca}(\text{NO}_3)_2$ and $\text{Ba}(\text{NO}_3)_2$. Namely, the thicknesses of PAH/PSS multilayers exposed to Ca^{2+} and Ba^{2+} ions were the same. Contrary to the divalent cations, Dressick and colleagues^[29] observed the ion-specific influence of divalent anions on the properties of PAH/PSS multilayers. However, in their study, divalent ions were present in the polyelectrolyte deposition solutions. Obviously, the pretreatment of PEMs with salt solution is more specific to the ion used than the post-treatment with salt. That is not so unusual considering that, as explained earlier, ionic specificity originates from the adsorption of polyelectrolytes on the surface, and this process largely depends on the conformation of the polyelectrolytes in solution.

In the end, it is interesting to consider how the type of divalent metal cation affects the composition of the PDADMAC/PSS multilayer. Within the multilayer, charged polyelectrolyte groups can be compensated either by oppositely charged polyelectrolyte repeating units ("intrinsic charge compensation") or by small counterions ("extrinsic charge compensation").^[52] The ion content of PEM markedly depends on the number of extrinsically compensated sites. In addition to ions, polyelectrolyte films contain a significant amount of water.^[53] Increasing the ion content in PEM usually increases water content as the ions carry water into the film.^[54,55] By considering cation hydration, bonding ability, and mode of binding, a rationalization of the difference between the ion (and water) content of films prepared in different supporting electrolytes may be reached. As Ni^{2+} , Zn^{2+} , and Cu^{2+} ions have similar degrees of hydration in solution (Table 1), the ion and water content of PEMs prepared in the presence of those transition metal cations should be alike. On the contrary, both ion and water content of the PDADMAC/PSS

multilayer should depend on the type of alkaline earth cation present in the polyion deposition solutions. Among Mg^{2+} , Ca^{2+} , and Sr^{2+} , the LbL assembly prepared in the presence of Mg^{2+} should have the lowest amount of extrinsically compensated sites and water because that ion has the lowest hydration shell and binding affinity. Between Ca^{2+} and Sr^{2+} ions, it is difficult to say which will be more effective in doping the PEM with ions and water. On the one hand, Ca^{2+} ions are less hydrated in solution than Sr^{2+} ions (Table 1), but on the other hand, Ca^{2+} ions are predominantly bound to PSS segments by ion bridges.

5. Conclusions

The influence of a supporting divalent cation on the properties of PDADMAC/PSS multilayer was studied using ellipsometry, AFM, and tensiometry. We have observed that cations of alkaline earth metals (Mg^{2+} , Ca^{2+} , and Sr^{2+}) affect the thickness and surface roughness of the PDADMAC/PSS film, whereas cations of transition metals (Ni^{2+} , Zn^{2+} , and Cu^{2+}) do not. The difference in the behavior of these two classes of cations was reasonably well explained by the difference in hydration of these ions. As the studied cations of transition metals are well and equally hydrated in solution, they will screen the charge of PSS repeating units in the same proportion. In contrast to cations of d-block elements, the hydration degree of investigated alkaline earth cations is lower and depends on the size of a cation. Consequently, PSS monomers will bind those cations with different affinity. As the conformation of macroion chains strongly depends on the number of associated counterions, the deposited mass of polyelectrolyte during the LbL process will vary depending on the used alkaline earth cation. In addition, the results of our experiments suggest that bridging of polyelectrolyte chains with divalent cations is also a significant factor in the assembly of LbL films. The obtained differences in the thickness and surface roughness of the PDADMAC/PSS multilayer prepared with solutions containing Ca^{2+} and Sr^{2+} ions were explained by the difference in the bridging ability of the PSS chains with the respective cations.

The ability to control the structure, content, and properties of PEMs by altering the nature of divalent cation present in the deposition solutions suggests the possibility of creating thin films for diverse applications ranging from membranes and sensors to biomedicine nanocarriers. Such tuning of multilayer properties by ion specificity is not limited to divalent cations but could also occur with trivalent cations. Therefore, we plan to additionally explore how the type of trivalent cation affects PEM properties.

Supporting Information

Photographs of PSS solutions prepared in the presence of MgCl_2 , CaCl_2 , SrCl_2 , NiCl_2 , CuCl_2 , ZnCl_2 , and BaCl_2 at salt concentrations of 0.1 and 0.5 mol dm^{-3} , effective hydrodynamic diameter of particles present in PSS solutions that contain different background

salts of 0.1 and 0.5 mol dm⁻³ concentration, and optical micrographs of (PDADMAC/PSS)₅ and (PDADMAC/PSS)₁₅ multilayers prepared in the presence of different supporting electrolytes.

Acknowledgements

The authors thank J. Nikolić for helpful discussions and assistance with LbL robot. This research was supported by the Croatian Science Foundation under the project IPS-2020-01-6126 and by infrastructural project CluK (KK.01.1.1.02.0016) from the European Regional Development Fund.

Conflict of Interests

The authors declare no conflict of interest.

Data Availability Statements

The data that support the findings of this study are available from the corresponding author upon reasonable request.

Keywords: Divalent cations · Polyelectrolyte multilayers · Polyelectrolytes · Specific ion effects

- [1] G. Decher, J. D. Hong, J. Schmitt, *Thin Solid Films* **1992**, 210–211, 831–835.
- [2] D. V. Andreeva, E. V. Skorb, D. G. Shchukin, *ACS Appl. Mater. Interfaces* **2010**, 2, 1954–1962.
- [3] D. M. Reurink, E. te Brinke, I. Achterhuis, H. D. W. Roesink, W. M. de Vos, *ACS Appl. Polym. Mater.* **2019**, 1, 2543–2551.
- [4] E. te Brinke, D. M. Reurink, I. Achterhuis, J. de Grooth, W. M. de Vos, *Appl. Mater. Today* **2020**, 18, 100471.
- [5] G. Laufer, C. Kirkland, A. B. Morgan, J. C. Grunlan, *Biomacromolecules* **2012**, 13, 2843–2848.
- [6] O. Köklükaya, F. Carosio, J. C. Grunlan, L. Wågberg, *ACS Appl. Mater. Interfaces* **2015**, 7, 23750–23759.
- [7] Q. Zhang, J. R. Smith, L. V. Saraf, *IEEE Sens. J.* **2009**, 9, 854–857.
- [8] X. Zhu, D. Jańczewski, S. Guo, S. S. C. Lee, F. J. P. Velandia, S. L.-M. Teo, T. He, S. R. Puniredd, G. J. Vancso, *ACS Appl. Mater. Interfaces* **2015**, 7, 852–861.
- [9] K. Bohinc, L. Kucic, R. S'tukelj, A. Zore, A. Abram, T. Klac'ic, D. Kovac'evic, *Coatings* **2021**, 11, 630.
- [10] A. J. Chung, M. F. Rubner, *Langmuir* **2002**, 18, 1176–1183.
- [11] T. Klac'ic, N. Peranic, B. Radatovic, D. Kovačević, *Colloids Surf., A* **2022**, 648, 129385.
- [12] S. S. Shiratori, M. F. Rubner, *Macromolecules* **2000**, 33, 4213–4219.
- [13] R. A. McAloney, M. Sinyor, V. Dudnik, M. Cynthia Goh, *Langmuir* **2001**, 17, 6655–6663.
- [14] E. Guzmán, H. Ritacco, J. E. F. Rubio, R. G. Rubio, F. Ortega, *Soft Matter* **2009**, 5, 2130–2142.
- [15] M. Lundin, F. Solaqa, E. Thormann, L. Macakova, E. Blomberg, *Langmuir* **2011**, 27, 7537–7548.
- [16] J. B. Schlenoff, M. Li, *Ber. Bunsenges. Phys. Chem.* **1996**, 100, 943–947.
- [17] S. T. Dubas, J. B. Schlenoff, *Macromolecules* **1999**, 32, 8153–8160.
- [18] K. Büscher, K. Graf, H. Ahrens, C. A. Helm, *Langmuir* **2002**, 18, 3585–3591.
- [19] M. Salomäki, I. A. Vinokurov, J. Kankare, *Langmuir* **2005**, 21, 11232–11240.
- [20] O. Guillaume-Gentil, R. Zahn, S. Lindhoud, N. Graf, J. Vörös, T. Zambelli, *Soft Matter* **2011**, 7, 3861–3871.
- [21] M. Mesić, T. Klac'ic, A. Abram, K. Bohinc, D. Kovačević, *Polymers* **2022**, 14, 2566.
- [22] M. Salomäki, P. Tervasmäki, S. Areva, J. Kankare, *Langmuir* **2004**, 20, 3679–3683.
- [23] M. Salomäki, T. Laiho, J. Kankare, *Macromolecules* **2004**, 37, 9585–9590.
- [24] M. Salomäki, J. Kankare, *Macromolecules* **2008**, 41, 4423–4428.
- [25] J. E. Wong, H. Zastrow, W. Jaeger, R. von Klitzing, *Langmuir* **2009**, 25, 14061–14070.
- [26] X. Zan, D. A. Hoagland, T. Wang, B. Peng, Z. Su, *Polymer* **2012**, 53, 5109–5115.
- [27] T. Klac'ic, K. Bohinc, D. Kovačević, *Macromolecules* **2022**, 55, 9571–9582.
- [28] R. von Klitzing, J. E. Wong, W. Jaeger, R. Steitz, *Curr. Opin. Colloid Interface Sci.* **2004**, 9, 158–162.
- [29] W. J. Dressick, K. J. Wahl, N. D. Bassim, R. M. Stroud, D. Y. Petrovykh, *Langmuir* **2012**, 28, 15831–15843.
- [30] O. Soltwedel, O. Ivanova, P. Nestler, M. Müller, R. Köhler, C. A. Helm, *Macromolecules* **2010**, 46, 7288–7293.
- [31] P. Nestler, M. Paßvogel, C. A. Helm, *Macromolecules* **2013**, 46, 5622–5629.
- [32] S. Doodoo, B. N. Balzer, T. Hugel, A. Laschewsky, R. von Klitzing, *Soft Mater* **2013**, 11, 157–164.
- [33] J. Fu, H. M. Fares, J. B. Schlenoff, *Macromolecules* **2017**, 50, 1066–1074.
- [34] M. Pourbaix, *Atlas of Electrochemical Equilibria in Aqueous Solutions*, National Association of Corrosion, Houston **1974**.
- [35] M. Kosmulski, *Surface Charging and Points of Zero Charge*, CRC Press, Boca Raton, Florida **2009**.
- [36] A. H. Al-Bayati, K. G. Orrman-Rossiter, J. A. van den Berg, D. G. Armour, *Surf. Sci.* **1991**, 241, 91–102.
- [37] M. Zerball, A. Laschewsky, R. von Klitzing, *J. Phys. Chem. B* **2015**, 119, 11879–11886.
- [38] J. W. Goodwin, *Colloids and Interfaces with Surfactants and Polymers—An Introduction*, Wiley, New Jersey **2009**.
- [39] S. Fujita, S. Shiratori, *Nanotechnology* **2005**, 16, 1821–1827.
- [40] D. Yoo, S. S. Shiratori, M. F. Rubner, *Macromolecules* **1998**, 31, 4309–4318.
- [41] M. Elzbiaciak, M. Kolasińska, P. Warszyński, *Colloids Surf. A* **2008**, 321, 258–261.
- [42] P. Kittitheeranun, S. T. Dubas, L. Dubas, *Appl. Mech. Mater.* **2012**, 229–231, 2745–2748.
- [43] R. von Klitzing, *Phys. Chem. Chem. Phys.* **2006**, 8, 5012–5033.
- [44] D. Volodkin, R. von Klitzing, *Curr. Opin. Colloid Interface Sci.* **2014**, 19, 25–31.
- [45] C. B. Bucur, Z. Sui, J. B. Schlenoff, *J. Am. Chem. Soc.* **2006**, 128, 13690–13691.
- [46] J. Fu, J. B. Schlenoff, *J. Am. Chem. Soc.* **2016**, 138, 980–990.
- [47] J. Požar, K. Bohinc, V. Vlasy, D. Kovačević, *Phys. Chem. Chem. Phys.* **2011**, 13, 15610–15618.
- [48] M. Elzbiaciak-Wodka, M. Kolasińska-Sojka, P. Warszyński, *J. Electroanal. Chem.* **2017**, 789, 123–132.
- [49] Y. Marcus, *Ion Properties*, Marcel Dekker Inc., New York **1997**.
- [50] J. Wei, D. A. Hoagland, G. Zhang, Z. Su, *Macromolecules* **2016**, 49, 1790–1797.
- [51] T. H. Silva, V. Garcia-Morales, C. Moura, J. A. Manzanares, F. Silva, *Langmuir* **2005**, 21, 7461–7467.
- [52] J. B. Schlenoff, H. Ly, M. Li, *J. Am. Chem. Soc.* **1998**, 120, 7626–7634.
- [53] T. Farhat, G. Yassin, S. T. Dubas, J. B. Schlenoff, *Langmuir* **1999**, 15, 6621–6623.
- [54] S. Doodoo, R. Steitz, A. Laschewsky, R. von Klitzing, *Phys. Chem. Chem. Phys.* **2011**, 13, 10318–10325.
- [55] J. B. Schlenoff, A. H. Rmaile, C. B. Bucur, *J. Am. Chem. Soc.* **2008**, 130, 13589–13597.

Manuscript received: February 27, 2025